Tools for laser spectroscopy: The design and construction of a Faraday isolator

S. Winter, C. Mok, and A. Kumarakrishnan

Abstract: We discuss the design and construction of a Faraday isolator for diode laser spectroscopy using commercially available components. The design involves modelling the magnetic field of an assembly of cylindrical magnets and verifying the predictions using a sensor. We obtain an isolation ratio for optical feedback of ∼35 dB at a wavelength of 780 nm. The cost is approximately one-fourth the cost of an equivalent commercially available device. We expect that the design can be widely used in experiments in laser spectroscopy and in advanced undergraduate laboratory experiments.

PACS Nos.: 01.50.Pa, 32.80.Pj, 39.25.+k, 42.62.Fi

Résumé : Nous discutons la conception et la construction d'un isolateur de Faraday pour la spectroscopie à diode laser en nous limitant à des composantes disponibles commercialement. La conception exige de modéliser le champ magnétique d'un assemblage d'aimants cylindriques et de vérifier ces prédictions à l'aide d'un senseur. Nous obtenons un rapport d'extinction de ∼35 dB à une longueur d'onde de 780 nm. Le coût est approximativement 25 % de celui d'un instrument vendu dans le commerce. Nous prévoyons que ce design sera largement utilisé par les expérimentateurs en spectroscopie laser et dans les laboratoires avancés de premier cycle.

[Traduit par la Rédaction]

1. Introduction

The Faraday effect is of interest in the context of a wide variety of phenomena. The Faraday rotation of radiation from pulsars in interstellar space is of astrophysical interest [1]. Faraday rotation can also be observed in liquids [2] and dilute atomic gases [3,4]. The effect has also been exploited for plasma diagnostics [5].

In experimental laser spectroscopy a device that is widely used and is known as a Faraday rotator utilizes this effect. The device consists of an optically active sample placed in a magnetic field. The plane of polarization of linearly polarized light incident on the sample undergoes a rotation through an angle that is proportional to the component of the magnetic field parallel to the direction of propagation of light, the length of the sample, and the rate of change of the index of refraction as a function of wavelength. An interesting application involves experiments with magneto-optical traps [6,7]. In these

S. Winter, C. Mok, and A. Kumarakrishnan.[1] Department of Physics, York University, 4700 Keele St. Toronto, ON M3J 1P3, Canada.

[1]Corresponding author (e-mail: akumar@yorku.ca).

experiments, it is useful to cancel the Earth's magnetic field and the field due to other magnetized materials at the location of the trapped cloud of atoms. This can be accomplished by exploiting Faraday rotation due to the trapped sample. A weak probe beam is aligned through the apparatus in the absence of the cold gas and is incident on a polarizing beam splitter. Light reflected and transmitted by the beam splitter is incident on two photodetectors and the difference in signal intensity recorded by these detectors serves as a reference. The rotation of the plane of polarization by the atomic cloud causes a change in signal intensity that can be used to cancel stray magnetic fields.

Placing a Faraday rotator (designed with a rotation angle of 45°) between two polarizers, whose axes are aligned to maximum transmission, creates an isolator or optical diode that allows the passage of light travelling in one direction, while blocking light that propagates in the opposite direction. Faraday isolators are often used inside the cavities of ring lasers [8]. In these lasers, counter-propagating beams travel in a closed loop through the cavity and their interaction with the gain medium leads to gain saturation. Isolators are used to block one of these beams and allow the amplified output from the cavity to propagate in a single direction.

Perhaps the most widely used application of a Faraday isolator pertains to the construction of optical diodes for diode lasers [9–11]. Optical diodes are used to protect lasers from optical feedback in the form of retro-reflected light from various optical elements. For experiments in which diode lasers play an important role such as in atom-trapping, the stability of the experiment is dependent on locking lasers to a specific atomic transition frequency. The presence of optical feedback can cause unwanted frequency shifts, and can even cause permanent damage to the laser diode [12].

It is not immediately obvious that a Faraday isolator is essential for eliminating optical feedback. A simple and inexpensive isolator can be created using a polarizing beam splitter that transmits horizontally polarized light and a $\lambda/4$ waveplate. Light from the laser is polarized horizontally after passing through the beam splitter and is circularly polarized by the waveplate. Retroreflections due to optical surfaces that result in opposite circular polarization are polarized vertically by the waveplate and blocked by the beam splitter. The isolation ratio of such a setup is determined by the extinction ratio of the beam splitter, and is usually of the order of 1000:1. However, this scheme fails if optical elements introduce any ellipticity in the retroreflected beam. In contrast, a Faraday isolator consists of an optically active crystal placed in a longitudinal magnetic field. The crystal is antireflection coated for the wavelength of interest to minimize losses, and placed between two polarizers. The first polarizer is aligned to transmit the laser light through the crystal. The plane of polarization is rotated by 45° in the crystal and the second polarizer is aligned to transmit the light passing through the crystal. When the retroreflected beam travels through the crystal, its plane of polarization is rotated in the same direction as that of the incoming beam. Since the light is then polarized perpendicular to its original direction, it is extinguished by the polarizer at the entrance of the isolator. This arrangement works even when optical elements introduce ellipticity in the retroreflected beam and emphasizes the advantage of using a Faraday isolator. These ideas can be confirmed on the basis of simple tests.

A wide range of isolators for a variety of wavelengths are commercially available and offer a range of extinction ratios for retroreflected light. The cost of a typical 35 dB isolator for CW lasers operating at ∼780 nm is ∼ $3000, with the cost scaling in proportion to the extinction ratio.

In this paper, we discuss the design and construction of an inexpensive Faraday isolator with an isolation ratio of ∼35 dB, which was built for under $1000. The basic design involves the use of permanent cylindrical magnets with a circular bore. The design produces a uniform magnetic field of ∼0.55 T over the length of the optically active medium, a terbium–gallium–garnet (TGG) crystal of length 19 mm that is antireflection coated for 780 nm.

The rest of the paper is organized as follows. Section 2 describes the theory of the Faraday effect and presents a mathematical model that explains the design. Section 3 describes the design parameters and method of construction. In Sect. 4, we present the results and conclude with a discussion of possible improvements to the design.

2. Theory

2.1. The Faraday effect

The physical origin of the off-resonant Faraday effect [3] can be understood by considering the orbital motion of an electron in a dielectric material in the presence of a magnetic field, B, applied perpendicular to the plane of orbit [13]. The characteristic angular frequency of the electron is the cyclotron frequency, $\omega_c = eB/m$, where m is the mass of the electron and e is the electron charge. This frequency, as well as the orbital radius, are modified depending on whether the incident light, with angular frequency ω, is right or left circularly polarized. The two orbital radii for opposite circular polarizations correspond to different dipole moments, which, in turn, give rise to different indices of refraction for the two polarizations. When linearly polarized light is incident on the dielectric, it can be considered as the superposition of right and left circularly polarized components. The two components travel through the medium with different phase velocities and experience a relative phase shift. As a result, the plane of polarization is rotated through an angle, β, given by ref. 4

$$\beta = \left(\frac{2\pi}{\lambda}\right)\left(\frac{n_r - n_l}{2}\right)d \tag{1}$$

Here, d is the thickness of the dielectric, λ is the wavelength of the light, and n_r and n_l are the indices of refraction for right and left circularly polarized light, respectively. The direction of rotation depends only on the direction of the magnetic field and not on the direction of propagation of light through the dielectric material. As a result, retroreflected light will be rotated through an angle equal to 2β.

To derive an expression for the Faraday rotation in a dielectric, we can model the optically active medium as a collection of harmonic oscillators, which are excited off-resonance by the driving field. The equation of motion for such a system is

$$m\frac{d^2x}{dt^2} + m\omega_0^2 x(t) = eE(t) \tag{2}$$

where ω_0 is the natural frequency of the system, ω is the driving frequency, $E(t)$ is the electric field, and $x(t)$ is the time-dependent position. The electric field and position can be written as

$$E(t) = E_0\,e^{-i\omega t} \tag{3}$$

and

$$x(t) = x_0\,e^{-i\omega t} \tag{4}$$

respectively. Using (3) and (4) we find that

$$x(t) = \frac{eE_0/m}{\omega^2 - \omega_0^2} \tag{5}$$

The polarization P of a dielectric can be expressed as

$$P = eNx(t) = (\varepsilon - \varepsilon_0)E(t) \tag{6}$$

where N is the number of electrons per unit volume, ε_0 is the permittivity of free space, and ε is the relative permittivity of the dielectric. Using (5), it can be shown that

$$\frac{\varepsilon}{\varepsilon_0} = 1 + \frac{Ne^2}{\varepsilon_0 m_e}\frac{1}{\omega_0^2 - \omega^2} \tag{7}$$

The frequency-dependent index of refraction is, therefore,

$$n = \sqrt{1 + \frac{N\,e^2}{\varepsilon_0 m_e} \frac{1}{\omega_0^2 - \omega^2}} \tag{8}$$

Solving (2) with an additional term for the force due to the magnetic field, it can be shown that the indices of refraction for right and left circular polarizations in the presence of a magnetic field are

$$n_{r,l} = \sqrt{1 + \frac{N\,e^2}{\varepsilon_0 m} \frac{1}{\left(\omega_0^2 - \omega^2\right) \mp eB\omega/m}} \tag{9}$$

The difference between the two indices of refraction can be approximated to give

$$n_r - n_l = \frac{N\,e^3 B\omega}{\varepsilon_0 m^2} \frac{1}{\left(\omega_0^2 - \omega^2\right)^2 - \left(\frac{qB\omega}{m}\right)^2} \tag{10}$$

Since we are considering the far-off resonance case, and since the cyclotron frequency is much smaller than the optical frequency associated with the driving field, we assume that

$$\left(\frac{qB}{m}\right)^2 \ll \frac{\left(\omega_0^2 - \omega^2\right)^2}{\omega^2}$$

and (10) can be reduced to

$$n_r - n_l = \frac{N\,e^3 B\omega}{\varepsilon_0 m^2} \frac{1}{\left(\omega_0^2 - \omega^2\right)^2} \tag{11}$$

Since

$$\frac{dn}{d\lambda} = \frac{dn}{d\omega} \frac{d\omega}{d\lambda}$$

we can use (8) to show that

$$\frac{dn}{d\lambda} = \frac{N\,e^2 \omega}{\varepsilon_0 m} \frac{1}{\left(\omega_0^2 - \omega^2\right)^2} \frac{2\pi c}{\lambda^2} \tag{12}$$

Comparing (11) and (12), we find that

$$n_r - n_l = \left(\frac{\lambda^2}{c}\right) \left(\frac{dn}{d\lambda}\right) \left(\frac{eB}{2\pi m}\right) \tag{13}$$

Equation (13) can be used in (1) to obtain an expression for the angle of rotation of the plane of polarization of incident light

$$\beta = \left(\frac{e}{2m} \frac{\lambda}{c} \frac{dn}{d\lambda}\right) Bd \tag{14}$$

Here, from ref. 14, the Verdet constant of the material can be defined as

$$V = \left(\frac{e}{2m} \frac{\lambda}{c} \frac{dn}{d\lambda}\right)$$

so that the expression for the angle of rotation becomes

$$\beta = BVd \tag{15}$$

The angle of rotation is therefore dependent only on the strength of the magnetic field, the length of the dielectric, and the wavelength and dispersion of the incident light.

Fig. 1. Figure at left shows the location of a single magnet in the chosen coordinate system. The figure at right represents the arrangement of dipoles used to model the magnetic field in the xz plane. The thick arrows represent two parallel dipoles. The magnetic field through the bore of a single magnet is modelled as the z-component of the magnetic field of two such dipoles along the z-axis.
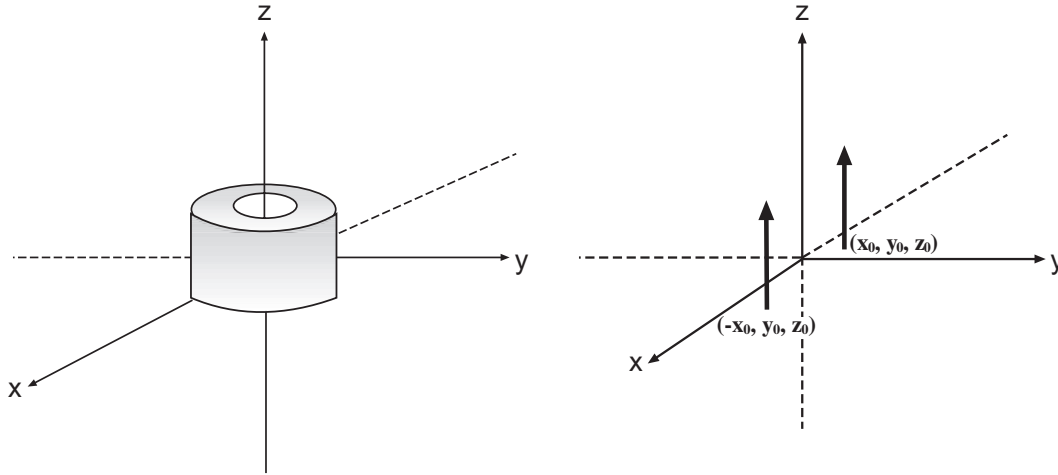
2.2. Mathematical model of the magnetic field

The design of a Faraday isolator has to ensure that a uniform magnetic field parallel to the direction of propagation of light is present over the length of the crystal. In practice, this can be achieved by using permanent cylindrical magnets with a circular bore. A single magnet can be considered to be the superposition of a regularly spaced array of parallel magnetic dipoles distributed around the axis of symmetry as shown in Fig. 1. To represent the magnetic field in the xz plane it is sufficient to consider the superposition of the field of two dipoles located equidistantly from the axis of symmetry. This axis can be defined as the z-axis as shown in Fig. 1. A disadvantage of this model is that is does not take into account the size of the dipoles. Another drawback is that the field inside the magnet, which has an effect on the field outside, is not calculated. Nevertheless, a system of dipoles can be used to model the main features of the magnetic field along the axes of the magnets used in the isolator.

For a single dipole located at the origin of a coordinate system, the equation for the magnetic field in spherical polar coordinates can be written in terms of the magnetic dipole moment, m, as [15]

$$B(r) = \frac{\mu_0 m}{4\pi r^3} \left(2\cos\theta \hat{r} + \sin\theta \hat{\theta} \right) \tag{16}$$

where unit vectors along r, θ, and ϕ are defined by

$$\hat{r} = \sin\theta\cos\theta\hat{x} + \sin\theta\cos\phi\hat{y} + \cos\theta\hat{z} \tag{17}$$

$$\hat{\theta} = \cos\theta\cos\phi\hat{x} + \cos\theta\sin\phi\hat{y} - \sin\theta\hat{z} \tag{18}$$

$$\hat{\phi} = -\sin\phi\hat{x} + \cos\phi\hat{y} \tag{19}$$

The coordinate system is shown in Fig. 2.

In our model, we consider the z-component of the magnetic field, since the rotation of the plane of polarization in the Faraday effect is caused only by the component of the magnetic field parallel to the direction of propagation of light. The z-component of $B(r)$ is

$$B(z) = \frac{\mu_0 m}{4\pi r^3} \left(2\cos^2\theta - \sin^2\theta \right) \hat{z} \tag{20}$$

Fig. 2. Spherical polar coordinate system.
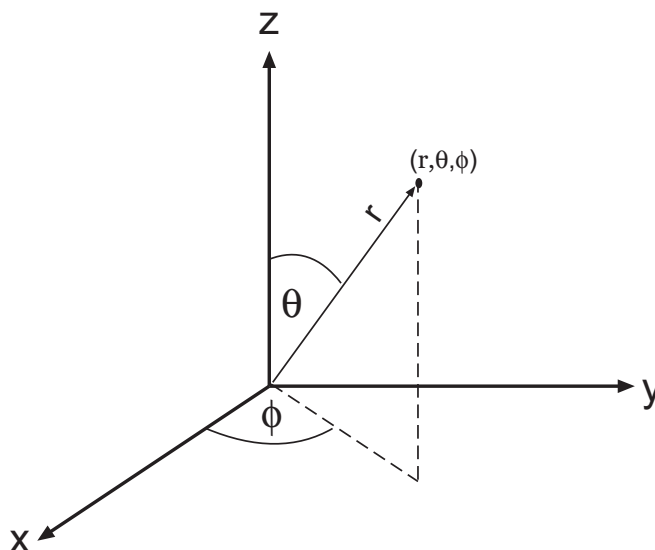
where

$$r = \sqrt{x^2 + y^2 + z^2} \tag{21}$$

and

$$\theta = \arctan \frac{\sqrt{x^2 + y^2}}{z} \tag{22}$$

If the dipole is located parallel to the z-axis, as shown in Fig. 1, (20) has to be modified to find the field along the axis of symmetry (z-axis). This is accomplished by replacing x, y, and z in (21) and (22) with $x \pm x_0$, $y \pm y_0$, and $z \pm z_0$. Here, (x_0, y_0, z_0) is the location of the dipole and (x, y, z) is the point on the axis of symmetry. The superposition of the field along this axis of symmetry for two parallel dipoles located on either side of the axis becomes

$$B(z) = \frac{\mu_0 m}{4\pi} \left[\frac{1}{r_1^3} \left(2\cos^2 \theta_1 - \sin^2 \theta_1 \right) + \frac{1}{r_2^3} \left(2\cos^2 \theta_2 - \sin^2 \theta_2 \right) \right] \hat{z} \tag{23}$$

where

$$r_1 = \sqrt{(x - x_0)^2 + (y - y_0)^2 + (z - z_0)^2}, \qquad \theta_1 = \arctan \frac{\sqrt{(x - x_0)^2 + (y - y_0)^2}}{(z - z_0)}$$

$$r_2 = \sqrt{(x + x_0)^2 + (y - y_0)^2 + (z - z_0)^2}, \qquad \theta_2 = \arctan \frac{\sqrt{(x + x_0)^2 + (y - y_0)^2}}{(z - z_0)} \tag{24}$$

Equations (23) and (24) represent the field of a single magnet. A plot of the magnetic field described by these equations is shown in Fig. 3. We assume that the distance of the dipoles with respect to the axis of symmetry is equal to the average diameter of the magnet used in the construction of the isolator. The absolute value of the field is scaled to match the measured field of the magnets. It is evident that the field that is predicted by the model represents the field along the symmetry axis of the magnet, which is the

Fig. 3. Plot shows the z-component of the magnetic field of a single cylindrical magnet based on (23) and (24).
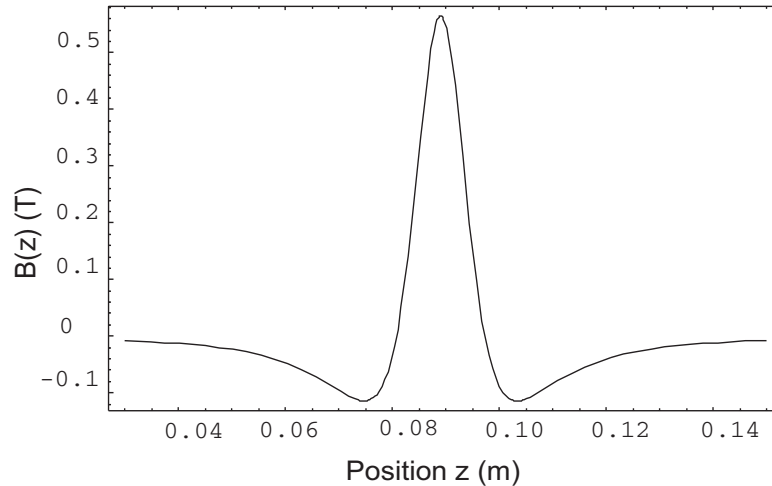

off-axis field of the system of dipoles. It can be seen that this off-axis field undergoes a zero crossing (change in the direction) by following the direction of the magnetic field lines. In contrast, the magnetic field along the axis of a dipole decreases as the distance from the centre of the dipole increases, without changing sign. As noted at the beginning of Sect. 2.2, the length of the dipoles is not considered.

3. Construction

3.1. Design parameters

The optically active material used is a TGG crystal, of length 19 mm and a diameter of 4.6 mm, that is antireflection coated for 780 nm. TGG was chosen because of its high Verdet constant of 75 rad T^{-1} m^{-1} at 780 nm. It can be estimated on the basis of (7) that the crystal should be placed in an average field of $\sim$0.55 T to produce a 45° rotation. Ideally, a single magnet with this magnetic field over the length of the crystal could be used in the isolator. However, our design is limited by the dimensions of commercially available magnets, which are cylindrical Nd–Be–Fe magnets with an outer diameter of 25 mm, an inner diameter of 6.625 mm, and a length of 11.25 mm. Based on measurements, the maximum magnetic field at the centre of a single magnet is 0.564 T. However, the average axial magnetic field along the length of the magnet is only 0.452 T. Although two magnets aligned pole to pole provide a field that acts in the same direction over the entire length of the crystal, the model described in Sect. 2, in which each magnet is represented by a ring of parallel dipoles, predicts that the field at the centre of two stacked magnets will be lower than the field at the centre of a single magnet. This can be seen by comparing Fig. 4*a*, which represents the expected field due to two magnets, to Fig. 3 (field of a single magnet). The reduced field at the centre is due to the change in direction of the magnetic field due to a single magnet. In Fig. 4*a*, the spatial coordinates were chosen to match the dimensions of the magnets. To increase the strength of the magnetic field at the centre, an additional magnet is added to either end of the assembly. The magnetic moments of the outer magnets oppose the directions of the magnetic moments of the inner magnets. A plot of the magnetic field of this arrangement based on the mathematical model in Sect. 2 is shown in Fig. 4*b*. This arrangement ensures that the magnetic field at the centre of the magnet assembly is uniform and that it has the value of 0.545 T across the length of the crystal. This is very nearly the same as the required value.

Fig. 4. Magnetic fields of magnet assemblies discussed in Sect. 3. (*a*) Model of magnetic field of two magnets with magnetic moments in the same direction. (*b*) Model of magnetic field of four magnets. The magnetic moments of the inner magnets point in the same direction, while those of the outer magnets point in the opposite direction.
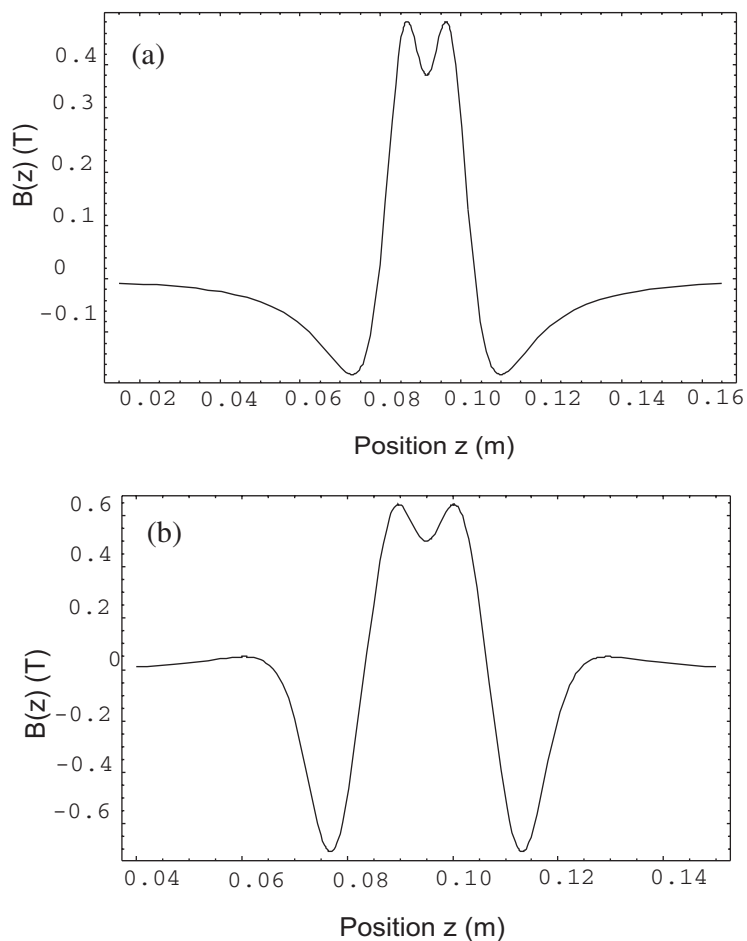
3.2. Assembly

The magnets are housed snugly in a cylindrical aluminum holder, shown in Fig. 5. The magnets are held in place by a cap that can be screwed on at one end. The main challenge involves assembling the two central magnets in the stack in a controlled manner to avoid shattering upon impact. This is accomplished using two Delrin wedges with slits that can be used to hold a cylindrical rod. The two magnets are placed on opposite ends of the rod, separated by the wedges. As the wedges are slowly slid apart, the magnets move closer together. The thinnest edge of each wedge is only a couple of millimetres in thickness, so when the wedges are completely removed, the magnets are sufficiently close so that the force with which they make contact is minimized. One of the magnets is placed in the aluminum holder and the two central magnets that are in contact and the fourth magnet are guided into place in the presence of the cylindrical rod and end cap. The crystal is fit snugly inside a Delrin tube (slightly longer than the TGG crystal), which is then slid into the centre of the magnet stack. The strength of the magnetic field over the crystal can be finely adjusted by changing the position of the crystal.

Fig. 5. Inside view of Faraday rotator. Arrows indicate the direction of the magnets in the holder.
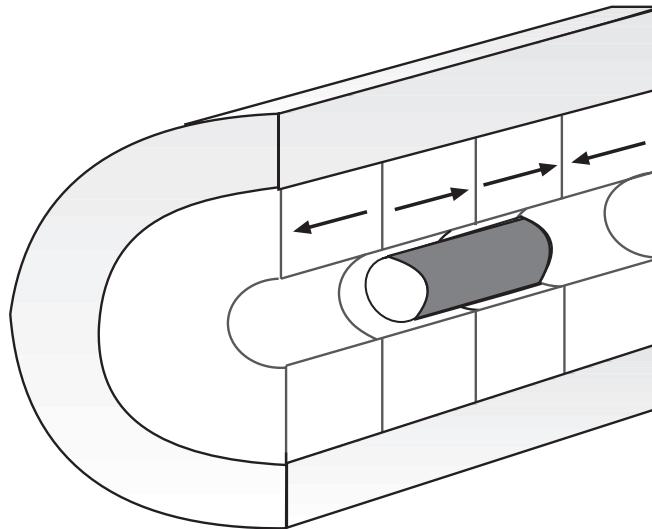

4. Results

The axial magnetic field through the bore of a single magnet was calibrated using a 4 mm × 2.3 mm Hall sensor with a sensitivity of 1×10^{-5} T. The 4 mm width of the sensor is approximately the same as the diameter of the laser beam used to test the optical isolation. We therefore assume that the sensor measurements represent the average magnetic field across the laser beam diameter. A plot of the axial magnetic field through the bore of a single magnet as a function of position is shown in Fig. 6a. Figure 6b shows the field in the presence of the two central magnets. Figure 6c shows the combined field of the entire magnet stack shown in Fig. 5. A multiparameter fit (continuous line) based on the model discussed in Sect. 2 is superposed on the data. The fit parameters x_0 and y_0 represent the distance of the probe from the dipoles and m is the effective magnetic moment. Four variables in the fit that are not specified include z_0, z_1, z_2, and z_3, which represent the locations of each pair of dipoles. These are not crucial parameters as they depend only on the choice of origin. The fits are in excellent agreement with the measured fields and can be compared with the predictions of the model in Figs. 3 and 4. The deviations of the fits from the data near the turning points are attributed to the assumptions in the model that ignore the spatial extent of the magnets and the contribution of the magnetization to the magnetic field.

Two sheet polarizers with an extinction ratio of approximately 10000:1 were used to measure the isolation ratio. The measured value of the isolation ratio IR was approximately 3500:1 (35 dB), which is generally adequate for isolating diode lasers from optical feedback. Tests with several isolators showed that the IR falls by approximately 2% if the laser beam diameter is varied between ∼2 mm and ∼4 mm. Additional tests were performed to characterize the sensitivity of the isolator with the position of the crystal and the alignment of the laser beam. The IR was measured as a function of the position of the TGG crystal and exhibits a Gaussian dependance (full width half maximum of approximately 8.7 mm) as a function of the displacement of the crystal from the centre of the magnet stack. The data suggest that the IR is degraded even if the crystal is displaced by a fraction of its length. Using a laser beam with a diameter of ∼2 mm, the IR was measured by translating the isolator perpendicular to the laser beam. In this case, the data show that the IR is relatively insensitive to the position and falls by approximately 5% for a displacement equal to half the diameter of the crystal. By changing the angle of the incoming beam relative to the axis of the crystal, it was determined that the isolation ratio is unchanged for an angular displacement up to 1°.

Fig. 6. Data points show the measured magnetic fields of the permanent cylindrical magnets. Continuous curves are the multiparameter fits based on the mathematical model. m represents the effective magnetic moment and $R = \left(x_0^2 + y_0^2\right)^{0.5}$ is the distance from the probe to the location of the pair of magnetic dipoles that model a magnet. The fit parameters x_0 and y_0 have uncertainties of $\pm 20\%$ and their values are consistent with the distance from the symmetry axis to the outer radii of the magnet. We do not specify the fit parameter z_0 since it depends only on the choice of the origin. (*a*) The magnetic field of a single magnet. $R = 10.5 \times 10^{-3}$ m and $m = 3.78$ A m^2. (*b*) The magnetic field of two magnets. $R = 11.5 \times 10^{-3}$ m and $m = 4.35$ A m^2. (*c*) The magnetic field of four magnets. $R = 11.8 \times 10^{-3}$ m and $m = 5.01$ A m^2.
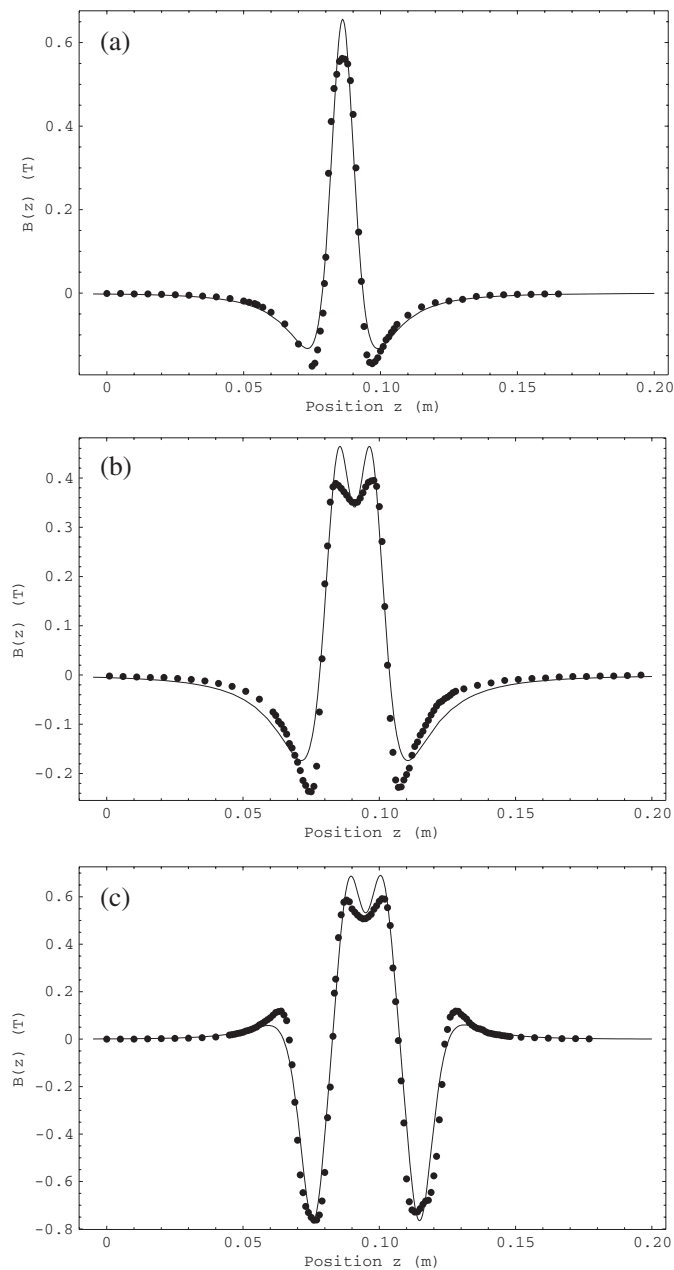
5. Summary

In summary, we have constructed a Faraday isolator with an isolation ratio of ∼35 dB. Apart from optical isolation for diode lasers used for research in atom trapping, the design can also be adapted to protect diode lasers used in advanced undergraduate laboratory experiments. The cost of a single unit was ∼$700. The cost and performance compare favourably with a commercially available device (∼$3000). We have also confirmed that a very simple model can be used to model the magnetic field of the magnet assembly. It is clear that the isolation ratio can be enhanced by using multiple isolators in series. From Fig. 6c, it is evident that two additional TGG crystals can be placed at the extrema of the magnetic field on either side of the central magnet stack. The lengths of the rods can be custom made to ensure that a uniform field is present across these crystals. This design will require additional waveplates to be inserted between the TGG rods. Nevertheless, it is realistic to expect isolation ratios of the order of 60 dB with such a design.

Acknowledgements

References

1. K.J. Gordon. Am. J. Phys. **46**, 530 (1978).
2. E.M. Briggs and R.W. Peterson. Am. J. Phys. **61**, 186 (1993).
3. D. Budker, D.J. Orlando, and V. Yashchuk. Am. J. Phys. **67**, 584 (1999).
4. D.A. Van Baak. Am. J. Phys. **64**, 724 (1996).
5. W.S. Porter and E.M. Bock, Jr. Am. J. Phys. **33**, 1070 (1965).
6. E.L. Raab, M. Prentiss, A. Cable, S. Chu, and D.E. Pritchard. Phys. Rev. Lett. **59**, 2631 (1987).
7. C. Monroe, W. Swann, H. Robinson, and C. Wieman. Phys. Rev. Lett. **65**, 1571 (1990).
8. A. Siegman. Lasers. University Science Books, Mill Valley, 1986.
9. C. Wieman, G. Flowers, and S. Gilbert. Am. J. Phys. **63**, 317 (1995).
10. K.B. MacAdam, A. Steinbach, and C. Wieman. Am. J. Phys. **60**, 1098 (1992).
11. C.E. Wieman and L. Hollberg. Rev. Sci. Instrum. **62**, 1 (1991).
12. W. Demtroder. Laser spectroscopy: Basic concepts and instrumentation. Springer Verlag, Berlin, 1981.
13. E. Hecht. Optics. Addison-Wesley, Reading, Mass. 2002.
14. F.L. Pedrotti and P. Bandettini. Am. J. Phys. **58**, 542 (1990).
15. D.J. Griffiths. Introduction to electrodynamics. Prentice Hall, Upper Saddle River. 1999.